APPLICATIONS OF HIGH-DIMENSIONAL TIME-DELAY EMBEDDING FOR TIME SERIES COMPLEXITY ESTIMATION

I. Morozov *†, Elettra-Sincrotrone Trieste S.C.p.A., Trieste, Italy
Yu. Maltseva Novosibirsk State Technical University, Novosibirsk, Russia

Abstract

Turn-by-turn (TbT) data are readily available in modern circular accelerators and are widely used to infer machine parameters in both simulations and experiments. In experiments, TbT data record transverse beam-centroid positions from beam position monitors (BPMs) and therefore include measurement noise. We construct high-dimensional time-delay embeddings of TbT time series, yielding matrix representations of transverse oscillation signals. Since the signals considered are typically near-quasiperiodic and dominated by harmonics of the fundamental betatron frequencies, the embedded matrices are expected to have low effective rank. We leverage this rank structure to define a complexity indicator based on singular-value spectra, which are related to the underlying quasiperiodic structure of the TbT signals. The proposed framework provides a simple, data-driven diagnostic for complexity estimation directly from TbT records and is compatible with experimental datasets.

INTRODUCTION

Modern circular particle accelerators are among the applications in which Hamiltonian, or symplectic, formalisms are successfully employed to model the experimentally observed dynamical behavior. During both the design stage and operation, significant effort is devoted to optimizing the dynamic aperture (DA) of a circular accelerator. The DA is a finite-time stability region in phase space, surrounding an elliptic fixed point, whose initial conditions remain bounded over a prescribed number of revolutions [1]. While the DA is a nontrivial object linked to the celebrated KAM [2] and Nekhoroshev [3] theorems, as well as Arnold diffusion [4], it is also of great practical importance for efficient beam injection and beam-lifetime optimization [5, 6].

The most reliable way to characterize the DA in simulations is the direct tracking of initial conditions within the domain of interest [7]. Together with DA scaling laws [8–11], direct computation makes it possible to extrapolate the DA size to long time scales for which direct numerical tracking is not feasible. Robust and computationally efficient methods for DA size and shape characterization can also be constructed using information from full unstable orbits [12, 13]. While these methods characterize the DA boundary, its internal structure remains unexplored. To characterize this structure, chaos indicators can be employed to determine whether a given initial condition is regular or chaotic. A family of chaos indicators can be constructed using information from tangent dynamics, such as the FLI [14] and GALI [15] indicators. The REM indicator [16] is instead based on the reversibility error obtained from the mismatch between forward and inverse iterations of a map. These methods are well suited for characterizing the internal structure of the DA [17]. FMA [18] is one of the most widely used chaos indicators in accelerator physics. It is based on the invariance of frequencies over time and also benefit from accelerated convergence using Birkhoff averages [19]. In contrast to many other indicators, FMA is based on TbT time-series analysis and can therefore be adapted to experimental data [20]. However, it is not necessarily ideal for the classification of initial conditions [21]. In practice, TbT signals represent beam-centroid transverse oscillations and are affected by measurement noise and beam decoherence.

In this contribution, we present a method for time-series complexity characterization based on the entropy of the SVD spectrum of high-dimensional time-delay embeddings of TbT signals [22]. Time-delay embedding represents a time series in a high-dimensional space of delayed coordinates [23], with Takens' theorem showing that such a representation preserves the geometrical structures relevant to the underlying dynamical system [24]. The singular-value spectrum of this representation can be used to characterize time-series complexity [25, 26] by means of Shannon entropy [27]. Data analysis based on this approach has been successfully applied in different fields, including finance [28] and biomedicine [29]. Motivated by the fast decay of harmonic content in regular quasiperiodic signals, we apply this method to the complexity characterization of TbT time series. The resulting indicator distinguishes structured regular signals, which have low effective complexity, from chaotic signals, which carry richer spectral information. We compare this method with several commonly used chaos indicators and study the effect of measurement noise.

HIGH-DIMENSIONAL EMBEDDING

The transverse dynamics in a circular accelerator can be modeled by the following 4D symplectic Hénon map:

$$
\begin{aligned}
q_x &\to \cos(\mu_x)\, q_x + \sin(\mu_x)\left(p_x + q_x^2 - q_y^2\right), \\
q_y &\to \cos(\mu_y)\, q_y + \sin(\mu_y)\left(p_y - 2q_x q_y\right), \\
p_x &\to \cos(\mu_x)\left(p_x + q_x^2 - q_y^2\right) - \sin(\mu_x)\, q_x, \\
p_y &\to \cos(\mu_y)\left(p_y - 2q_x q_y\right) - \sin(\mu_y)\, q_y,
\end{aligned}
$$

where (q_x, q_y, p_x, p_y) are the normalized transverse phase-space coordinates. In experimental measurements, only the transverse position coordinates q_x and q_y are available. The phase advances are given by $(\mu_x, \mu_y) = (2\pi\nu_x, 2\pi\nu_y)$, with betatron tunes $\nu_x = 0.168$ and $\nu_y = 0.201$.

* ivan.morozov@elettra.eu
† I.M. acknowledges support from the Elettra 2.0 project.

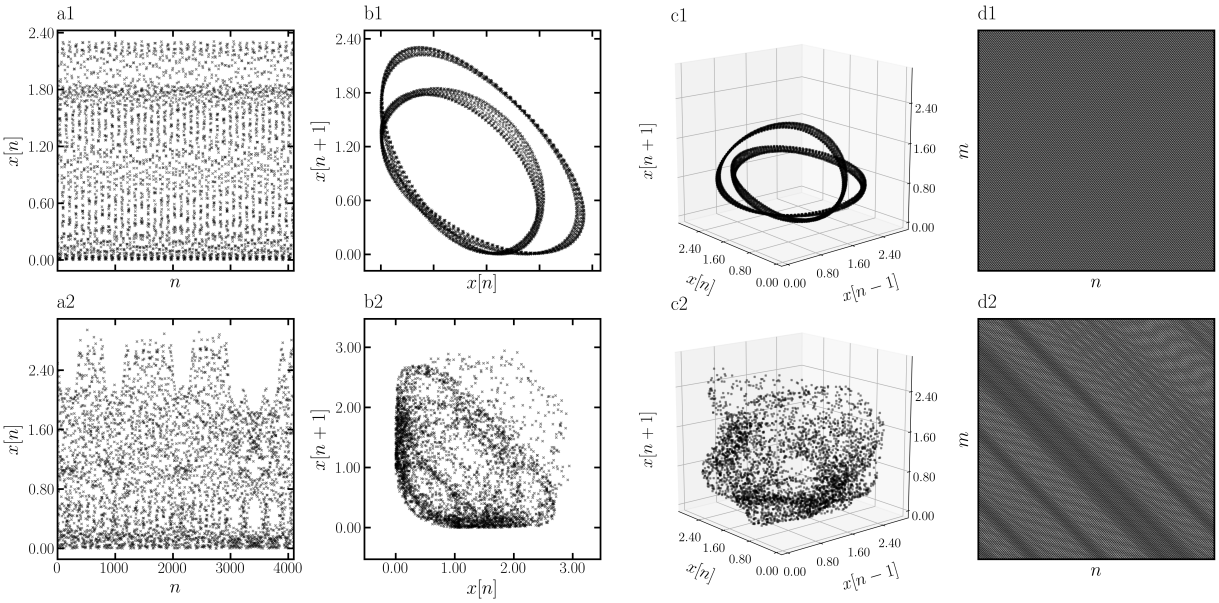

Figure 1: Examples of time-delay embeddings for regular (top row) and chaotic (bottom row) observables in one, two, and three dimensions (a1–c1 and a2–c2), together with their corresponding Hankel matrices (d1 and d2).

This map captures representative nonlinear effects present in more detailed lattice maps composed of individual magnet transformations, including finite stability, resonances, and chaos. Figure 2 shows the result of applying a GALI-based indicator in the (q_x, q_y) plane, together with projections of phase-space for regular and chaotic initial conditions.

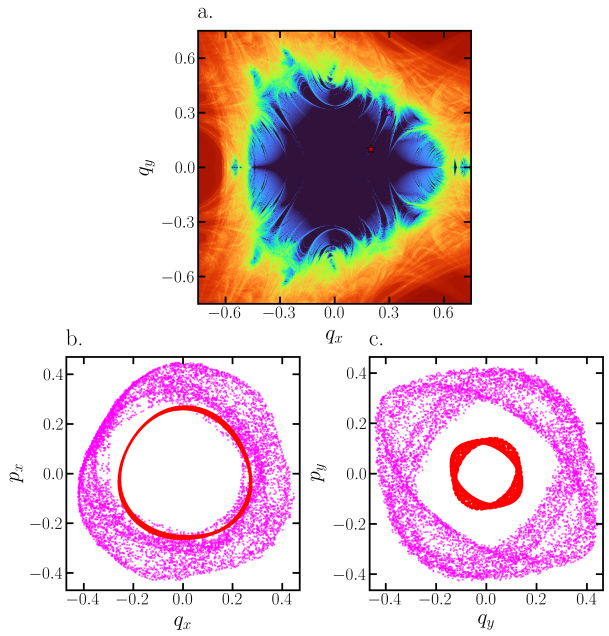

Figure 2: GALI indicator in the (q_x, q_y) plane (a) and phase-space trajectories for regular (red) and chaotic (magenta) initial conditions (b and c).

Given an initial condition, time series for the phase space coordinates can be generated by repeated application of the map. An observable $x(n) = f(q_x(n), p_x(n), q_y(n), p_y(n))$ can then be constructed, together with its corresponding time-delay representation, as illustrated in Figure 1. For a delay τ, an embedding dimension d, and a window length ℓ, the time-delay Hankel matrix is defined as

$$H = \begin{pmatrix} x_0 & x_\tau & x_{2\tau} & \cdots & x_{(\ell-1)\tau} \\ x_\tau & x_{2\tau} & x_{3\tau} & \cdots & x_{\ell\tau} \\ x_{2\tau} & x_{3\tau} & x_{4\tau} & \cdots & x_{(\ell+1)\tau} \\ \vdots & \vdots & \vdots & \ddots & \vdots \\ x_{(d-1)\tau} & x_{d\tau} & x_{(d+1)\tau} & \cdots & x_{(d+\ell-1-1)\tau} \end{pmatrix}.$$

HANKEL-SVD ENTROPY INDICATOR

We quantify the complexity of a scalar observable by constructing a time-delay Hankel embedding, computing its singular values, and evaluating the Shannon entropy of the normalized singular-value spectrum. Let $H = U\Sigma V^{\mathsf{T}}$ be the singular value decomposition of H, with singular values $\sigma_1, \sigma_2, \ldots, \sigma_r$, where $r = \min(d, \ell)$. The normalized singular-value spectrum is

$$p_i = \frac{\sigma_i}{\sum_{j=1}^{r} \sigma_j}, \qquad i = 1, \ldots, r.$$

The Hankel–SVD entropy indicator is then defined as the Shannon entropy of this spectrum,

$$S_{\mathrm{SVD}} = -\sum_{i=1}^{r} p_i \log_2 p_i,$$

or, in normalized form, $\hat{S}_{\mathrm{SVD}} = S_{\mathrm{SVD}} / \log_2 r$. Small values of $\hat{S}_{\mathrm{SVD}}$ indicate that the embedded signal is well described by a small number of dominant singular directions, whereas values close to one indicate a broad singular-value spectrum and therefore a more complex embedded time-series representation. An example of a normalized singular-value spectrum is shown in Figure 4 for regular and chaotic initial conditions.

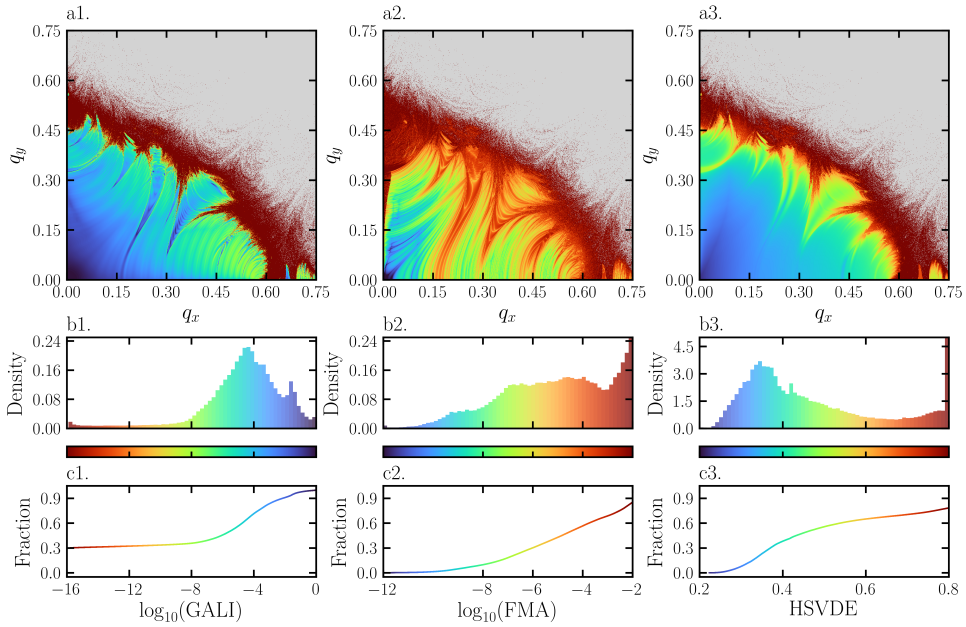

Figure 3: Application of the GALI (a1–c1), FMA (a2–c2), and HSVDE (a3–c3) indicators to a dense grid of initial conditions in the transverse (q_x, q_y) plane. Indicator distributions are shown in panels (b1–b3), and sorted indicator values are shown in panels (c1–c3).

Figure 3 shows the application of the GALI, FMA, and HSVDE indicators to a dense grid of initial conditions in the space of transverse coordinates. All indicators reveal the internal resonance structure, visible as feather-like patterns emerging from inside the stable region and extending toward its boundary, as well as the chaotic layer defining the stability boundary. The HSVDE indicator exhibits a structure similar to the mirrored GALI indicator and demonstrates a bimodal distribution, corresponding to regular and chaotic classes.

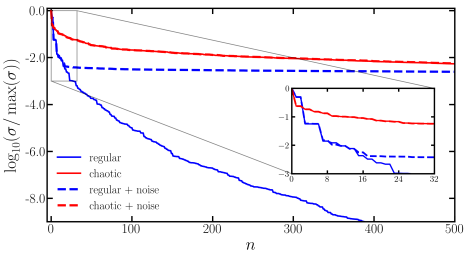

Figure 4: Example of a normalized singular-value spectrum for Hankel matrices constructed from regular (blue) and chaotic (red) initial conditions.

The effect of measurement noise is illustrated in Figure 5, where Gaussian noise with standard deviation $\sigma = 0.01$ was added to the generated signals before applying the FMA and HSVDE workflows. The signals were standardized, and $\hat{q}_x^2 + \hat{q}_y^2$ was used as the scalar time-series observable. No additional filtering or combination of frequency data from several BPMs was performed to improve the frequency-estimation accuracy of the FMA indicator. The same color range as in the noiseless case is used. As can be seen, while FMA still highlights the boundary and some of the internal resonance structures, the overall indicator range is reduced by the noise, and a noise-induced band appears at small amplitudes. The HSVDE indicator is also affected by noise, but the effect is less severe and appears near the boundary.

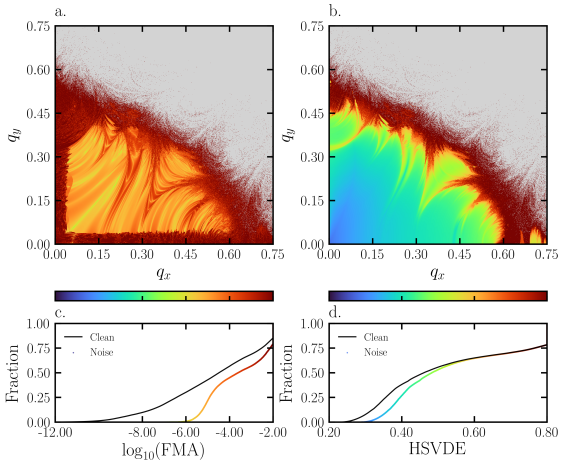

Figure 5: Application of FMA and HSVDE to the Hénon map with added noise. The sorted indicator values without noise are shown as solid black curves for comparison.

CONCLUSION

The application of the HSVDE chaos indicator, based on high-dimensional time-delay embedding of an observable constructed from TbT time series, has been presented. The indicator is straightforward to construct and is well motivated by the quasiperiodic structure of regular orbits. Similarly to the GALI indicator, HSVDE reveals internal DA geometric structures and is sensitive to chaotic initial conditions. A preliminary study with noisy signals demonstrates the robustness of the indicator, making it a promising candidate for experimental applications.

REFERENCES

[1] W. Scandale, "Dynamic aperture", CERN, Geneva, Switzerland, CERN-SL-94-24-AP, 1995. doi:10.5170/CERN-1995-006.109

[2] V. I. Arnold, "Small denominators and problems of stability of motion in classical and celestial mechanics", *Russian Mathematical Surveys*, vol. 18, no. 6, pp. 85–191, 1963. doi:10.1070/RM1963v018n06ABEH001143

[3] N. N. Nekhoroshev, "An exponential estimate of the time of stability of nearly-integrable hamiltonian systems", *Russian Mathematical Surveys*, vol. 32, no. 6, p. 1, 1977. doi:10.1070/RM1977v032n06ABEH003859

[4] "Instability of dynamical systems with several degrees of freedom", in *Collected Works: Representations of Functions, Celestial Mechanics and KAM Theory, 1957–1965*, A. B. Givental *et al.*, Eds. Berlin, Heidelberg: Springer Berlin Heidelberg, 2009, pp. 423–427. doi:10.1007/978-3-642-01742-1_26

[5] K. Oide *et al.*, "Design of beam optics for the future circular collider e^+e^- collider rings", *Phys. Rev. Accel. Beams*, vol. 19, no. 11, p. 111005, 2016. doi:10.1103/PhysRevAccelBeams.19.111005

[6] E. H. Maclean, R. Tomás, F. Schmidt, and T. H. B. Persson, "Measurement of nonlinear observables in the large hadron collider using kicked beams", *Phys. Rev. Spec. Top. Accel. Beams*, vol. 17, no. 8, p. 081002, 2014. doi:10.1103/PhysRevSTAB.17.081002

[7] E. Todesco and M. Giovannozzi, "Dynamic aperture estimates and phase-space distortions in nonlinear betatron motion", *Phys. Rev. E*, vol. 53, no. 4, pp. 4067–4076, 1996. doi:10.1103/PhysRevE.53.4067

[8] A. Bazzani, M. Giovannozzi, E. H. Maclean, C. E. Montanari, F. F. Van der Veken, and W. Van Goethem, "Advances on the modeling of the time evolution of dynamic aperture of hadron circular accelerators", *Phys. Rev. Accel. Beams*, vol. 22, no. 10, p. 104003, 2019. doi:10.1103/PhysRevAccelBeams.22.104003

[9] M. Giovannozzi, W. Scandale, and E. Todesco, "Dynamic aperture extrapolation in the presence of tune modulation", *Phys. Rev. E*, vol. 57, no. 3, pp. 3432–3443, 1998. doi:10.1103/PhysRevE.57.3432

[10] A. Bazzani, S. Marmi, and G. Turchetti, "Nekhoroshev estimate for isochronous non resonant symplectic maps", *Celestial Mech. Dyn. Astron.*, vol. 47, no. 4, pp. 333–359, 1989. doi:10.1007/BF00051010

[11] G. Turchetti, "Nekhoroshev stability estimates for symplectic maps and physical applications", in *Number Theory and Physics*, pp. 223–234, 1990.

[12] I. Morozov and M. Giovannozzi, "Estimating the Stability Domain of Symplectic Maps: A Robust Method via Bounding Set of Unstable Initial Conditions", presented at IPAC'26, Deauville, France, May 2026, paper WEP5028, this conference,

[13] I. Morozov, "domain", *GitHub repository*, 2026. https://github.com/i-a-morozov/domain

[14] C. Froeschlé, R. Gonczi, and E. Lega, "The fast lyapunov indicator: a simple tool to detect weak chaos. application to the structure of the main asteroidal belt", *Planet. Space Sci.*, vol. 45, no. 7, pp. 881–886, 1997. doi:10.1016/S0032-0633(97)00058-5

[15] C. Skokos, TC. Bountis, and C. Antonopoulos, "Geometrical properties of local dynamics in hamiltonian systems: the generalized alignment index (gali) method", *Physica D: Nonlinear Phenomena*, vol. 231, no. 1, pp. 30–54, 2007. doi:10.1016/j.physd.2007.04.004

[16] F. Panichi, L. Ciotti, and G. Turchetti, "Fidelity and reversibility in the restricted three body problem", *Commun. Nonlinear Sci. Numer. Simul.*, vol. 35, pp. 53–68, 2016. doi:10.1016/j.cnsns.2015.10.016

[17] T. Zolkin, S. Nagaitsev, I. Morozov, S. Kladov, and Y.-K. Kim, "Isochronous and period-doubling diagrams for symplectic maps of the plane", *Chaos, Solitons & Fractals*, vol. 198, p. 116513, 2025. doi:10.1016/j.chaos.2025.116513

[18] J. Laskar, "Frequency map analysis and quasiperiodic decompositions", Jun. 2003. doi:10.48550/arXiv.math/0305364

[19] S. Das and J. A. Yorke, "Super convergence of ergodic averages for quasiperiodic orbits", *Nonlinearity*, vol. 31, no. 2, p. 491, Jan. 2018. doi:10.1088/1361-6544/aa99a0

[20] D. Robin, C. Steier, J. Laskar, and L. Nadolski, "Global dynamics of the advanced light source revealed through experimental frequency map analysis", *Phys. Rev. Lett.*, vol. 85, no. 3, pp. 558–561, 2000. doi:10.1103/PhysRevLett.85.558

[21] A. Bazzani, M. Giovannozzi, C. E. Montanari, and G. Turchetti, "Performance analysis of indicators of chaos for nonlinear dynamical systems", *Phys. Rev. E*, vol. 107, no. 6, p. 064209, 2023. doi:10.1103/PhysRevE.107.064209

[22] I. Morozov, "tohubohu", *GitHub repository*, 2025. https://github.com/i-a-morozov/tohubohu

[23] N. H. Packard, J. P. Crutchfield, J. D. Farmer, and R. S. Shaw, "Geometry from a time series", *Phys. Rev. Lett.*, vol. 45, no. 9, pp. 712–716, Sep. 1980. doi:10.1103/PhysRevLett.45.712

[24] F. Takens, "Detecting strange attractors in turbulence", in *Dynamical Systems and Turbulence, Warwick 1980*, pp. 366–381, 1981.

[25] DS. Broomhead and G. P. King, "Extracting qualitative dynamics from experimental data", *Physica D: Nonlinear Phenomena*, vol. 20, no. 2, pp. 217–236, 1986. doi:10.1016/0167-2789(86)90031-X

[26] R. Vautard and M. Ghil, "Singular spectrum analysis in nonlinear dynamics, with applications to paleoclimatic time series", *Physica D: Nonlinear Phenomena*, vol. 35, no. 3, pp. 395–424, 1989. doi:10.1016/0167-2789(89)90077-8

[27] C. E. Shannon, "A mathematical theory of communication", *Bell System Technical Journal*, vol. 27, no. 3, pp. 379–423, 1948. doi:10.1002/j.1538-7305.1948.tb01338.x

[28] J. Alvarez-Ramirez and E. Rodriguez, "A singular value decomposition entropy approach for testing stock market efficiency", *Physica A: Statistical Mechanics and its Applications*, vol. 583, p. 126337, 2021. doi:10.1016/j.physa.2021.126337

[29] A. Marin-Lopez, F. Martinez-Martinez, J. A. Martinez-Cadena, and J. Alvarez-Ramirez, "Multiscale SVD entropy for the analysis of gait dynamics", *Biomedical Signal Processing and Control*, vol. 87, p. 105439, 2024. doi:10.1016/j.bspc.2023.105439